Modeling the Mechanical Properties of Notched Aluminum—Epoxy Particulate Composites

G.C. Papanicolaou, A.G. Xepapadaki, G.A. Angelakopoulos

Composite Materials Group, Department of Mechanical and Aeronautical Engineering, University of Patras, Patras 26500, Hellas

Received 17 November 2011; accepted 13 January 2012
DOI 10.1002/app.36823
Published online in Wiley Online Library (wileyonlinelibrary.com).

ABSTRACT: The aim of the present investigation is to study both the influence of particle weight fraction (0–50%) and the effect of the notch length on the static mechanical properties of aluminum particle epoxy composites. Experimental results in both cases were compared with three different theoretical models, previously developed by the first author and presented in a series of publications. First, for the evaluation of the maximum strength the particle sectioning model (PSM) was applied. Next, for the evaluation of the elastic modulus as a function of aluminum powder weight fraction, the interphase model (IM) was applied. Finally, in the case of notches' length influence, the residual property model, (RPM), was applied. This model can be applied for the description of the residual behavior of materials after any type of damage. In all cases, predicted values showed a satisfactory agreement with experimental findings.
 J Appl Polym Sci 000: 000–000, 2012

Key words: degradation; fracture; interfaces; mechanical properties; modeling

INTRODUCTION

The use of composite materials in engineering applications is rapidly growing, mainly because of their specific high strength and their good resistance to corrosion and weathering. Their performance in structures compete the one of the traditional materials, such as metals, wood, etc. A composite system usually consists of stiff inclusions, embedded in a soft matrix with completely different elastic properties. During processing there is a third phase developed between the prime constituents, and the elastic properties of this phase depend on those of the prime materials.

The present work is an effort to study the static bending behavior of aluminum-filled epoxy particulate composites with and without notches and also to correlate experimental results with respective theoretical predictions based on micromechanics.[1–12] Several semi-empirical models/expressions developed by Papanicolaou et al. and by others were used and their predictions were also compared with respective experimental results.[13–26]

First, for the evaluation of the maximum strength the particle sectioning model (PSM) was applied.[13] According to this model, each particle is divided into an infinite number of coaxial cylinders and by applying Cox's theory the mean stress developed in each section of the particle may be calculated. Next, for the evaluation of the elastic modulus as a function of aluminum powder weight fraction, the interphase model was applied.[14] This model takes into account the existence of an interphase developed between the two main phases. The interphase constitutes an important parameter influencing the behavior of any composite material. The interphase layer which is developed in the area between the matrix and filler is characterized by different physico-chemical properties from those of the constituent phases and variable ones along its thickness. Predicted values were in satisfactory agreement with almost all percentages of aluminum particles.Finally, in the case of notches' length influence, the residual property model (RPM) was applied. This model can be applied for the description of the residual behavior of materials after damage. As it has already been proved in previous publications, the model gives satisfactory predictions for the residual materials properties variations irrespectively of the cause of damage and the type of the material considered at the time.[15]

PREDICTIVE MODELS

Predictive models for the elastic modulus

The mechanical properties of particulate-filled composites are affected by a great number of geometrical, topological, mechanical, etc. parameters. Numerous past studies have been focused on the

Correspondence to: G.C. Papanicolaou (gpapan@mech.upatras.gr).

micromechanics of particulate filled composites.[16–26] Unfortunately, the discrepancies between theoretical predictions and experimental data continue to limit the understanding of these composite materials. In all existing theories, difficulty has been encountered in separating such variables as interfacial adhesion, particle agglomeration, dispersion, and particle shape, all of which affect mechanical behavior. Other parameters such as polymerization-induced stresses and shear effects around filler particles complicate further the prediction.[13–28]

The oldest existing theory refers to inclusions in a viscous matrix and was developed by Einstein.[16] He considered rigid spherical non-solvated particles in a Newtonian viscous fluid and his final expression for the prediction of the effective modulus of the particulate composite is:

$$\frac{E_c}{E_m} = 1 + 2.5V_f \tag{1}$$

where E_c and E_m are the elastic moduli for the composite and the matrix, respectively, and V_f , the filler-volume fraction.

An extension of Einstein's equation is that developed by Guth and Smallwood.[17,18]

$$\frac{E_c}{E_m} = 1 + 2.5V_f + 14.1V_f^2 \tag{2}$$

Next, an equation based on a mathematical theory and valid for polymer-particulate composites when in glassy state is due to Kerner.[19] The final expression of this theory as applied to rigid fillers is:

$$\frac{E_c}{E_m} = 1 + \frac{V_f}{V_m}\left[\frac{15(1-v_m)}{8-10v_m}\right] \tag{3}$$

where v_m, is the matrix Poisson's ratio and V_m and V_f is the matrix and filler volume fraction, respectively.

The effect of filler agglomeration is taken into account in the following equation proposed by Mooney.[20]

$$\frac{E_c}{E_m} = \exp\left(\frac{2.5V_f}{1-sV_f}\right) \tag{4}$$

where s is a "crowding factor" taking values in the range 1 to 2 depending on the type of particle distribution into the polymer matrix. For closely packed spheres of uniform size, $s = 1.35$.

Another equation is that proposed by Eilers and Van Dyck[21]:

$$\frac{E_c}{E_m} = \left(1 + \frac{kV_f}{1-S'V_f}\right)^2 \tag{5}$$

where k and S' are constants usually equal to 1.25 and 1.20, respectively.

Phillips suggested the following expression for the Young's modulus of particulate composites assuming a simple model based on a cubic array of equivalent volume fraction to spherical particles dispersed in a continuous phase[22]:

$$\frac{E_c}{E_m} = \frac{X^2}{1 - X(1 - E_m/E_f)} + (1 - X^2) \tag{6}$$

X can be related to the volume fraction of the discontinuous phase, V_f, by an expression of the form:

$$X = (PV_f)^{1/3} \tag{7}$$

where P is a disposable parameter described as the "relative volume fraction," since it is the ratio: (volume of equivalent cubic particles)/(volume of spherical particles).

Phillips has shown that $P = 1$ for cubic particles, and that for spherical particles P is $6/\pi = 1.91$ and $2/\sqrt{3}\ \pi = 0.37$ for the upper and the lower bound, respectively.

Predictive models for the mechanical strength

In the case of a brittle thermoset polymer, such as epoxy or thermoset polyester, that has relatively low-fracture energy, the addition of fillers tends to increase the fracture toughness and the maximum strength at low filler weight fractions. However, above a critical volume fraction, both the fracture energy and the maximum strength decrease. The critical weight fraction at which the maximum fracture energy and/or the maximum strength are attained depends on the filler particle size as well as the interfacial bond between the fillers and the polymer matrix. The larger the particle size, the greater the critical volume fraction as well as the maximum fracture energy, although the effect of the latter is somewhat conflicting. The maximum strength of a filled polymer is more difficult to predict than the modulus. Unless there is a good bonding between the fillers and the polymer, the fillers do not share much load with the polymer; instead, they merely act as sources of stress concentration. In the case of no adhesion, the mechanical strength of the filled polymer decreases with increasing filler volume fraction.

There have also been reported some equations for estimating the tensile strength of particulate composites. One the most common equations concerning the composition dependence of mechanical properties of composites is Leidner and Woodhams equation[23]:

$$\sigma_{\mathrm{uc}} = 0.83P_\alpha V_b + K\sigma_{\mathrm{um}}(1 - V_b) \tag{8}$$

where: $P_\alpha = 10.62$ MPa, $K = 0.8$ or 0.9

Piggot and Leidner suggested the following equation[24]:

$$\sigma_{\mathrm{uc}} = \sigma_{\mathrm{um}}\left(1 - 0.5V_b^{0.6}\right) \quad (9)$$

Another equation was suggested by Nicolais and Mashelkar[25]:

$$\sigma_{\mathrm{uc}} = \sigma_{\mathrm{um}} - bV_b^n \quad (10)$$

where b is a constant, which can be assumed either positive or negative value.

And finally Schrager suggested[26]:

$$\sigma_{\mathrm{uc}} = \sigma_{\mathrm{um}} \exp(-2.66V_b) \quad (11)$$

In eqs. (8)–(11), σ_{um} is the ultimate strength of the matrix material; σ_{uc} is the maximum ultimate load carried by the composite and V_b is the filler volume fraction.

The interphase model

During manufacturing of particle-reinforced polymers (PRPs), interphases are developed lying at the close vicinity of the surface of reinforcing fillers. In common PRPs, these intermediate material phases have complex structure, contain voids, microcracks, and several impurities, while matrix macromolecules belonging to these areas are characterized by a reduced mobility. The interphase being separating the distinct filler and matrix phases is a region in which filler and matrix are mechanically and chemically combined or indistinct. It may be a diffusion zone or a chemical reaction zone and thus may be studied within the context of a composite material system that acts as a single entity. This system exists when two or more distinct materials interact synergistically to produce a superior material.

A theoretical model for the prediction of the elastic modulus and the Poisson's ratio of polymer matrix particulates which considers the existence of a particle-matrix inhomogeneous interphase has been developed by Papanicolaou et al.[27,28] According to this model, the interphase thickness Δr_i and the interphase volume fraction, V_i, is first calculated as:

$$\left(\frac{r_f+\Delta r_i}{r_f}\right)^3 - 1 = \frac{\lambda V_f}{1 - V_f}$$
$$V_i = \frac{3\Delta r_i V_f}{r_f} \quad (12)$$

where the parameter λ, is given by:

$$\lambda = 1 - \frac{\Delta C_p^{\mathrm{f}}}{\Delta C_p^0}$$
$$r_i = r_f + \Delta r_i \quad (13)$$

where r_f and r_i are the outer radii of the filler and the interphase, respectively.

In which ΔC_p^f and ΔC_p^0 correspond to the abrupt jump in heat capacity observed at the transition region for the filled and the unfilled polymer respectively.

Then the interphase Poisson's ratio, v_i and the composite Poisson's ratio, v_c can be calculated as:

$$v_i(r) = \frac{v_f - v_m}{(r_i - r_f)^2} r^2 + \frac{2(v_m - v_f)r_i}{(r_i - r_f)^2} r + \frac{v_f {r_i}^2 + v_m {r_f}^2 - 2v_m r_f r_i}{(r_i - r_f)^2} \quad (14)$$

$$v_c = v_f V_f + v_m V_m + v_i V_i, \quad (15)$$

Last equation can be written as:

$$v_c = v_f v_f + v_m V_m + \frac{3V_f}{{r_m}^3} \int_{r_f}^{r_i} v_i r^2 \, dr \quad (16)$$

Finally, the modulus of the composite, E_c, can be calculated by the relation:

$$\frac{(1 - 2v_c)}{E_c} = \frac{(1 + v_f)^2 (1 - 2v_m)^2}{(1 - 2v_f)(1 + v_m)^2} V_f + \frac{(1 - 2v_m)}{E_m} V_m + \frac{3(1 - 2v_m)^2 V_f}{(1 + 2v_m) r_f^3} \int_{r_f}^{r_i} \frac{(1 + v_i)^2}{(1 - 2v_i)E_i} r^2 \, dr \quad (17)$$

The particle sectioning model

In 1992, Papanicolaou et al. suggested a theoretical model that can predict the maximum stress of a composite reinforced with particles. According to this model, a discretization of a model spherical particle into infinite number of fibers was suggested (Fig. 1). Next, Coxs' theory for the calculation of fibers' stresses, for an applied stress on a random cross section, which is located at distance x from the center of a random fiber, i, having a fiber length of $2l_i$, was applied (Fig. 2). Stress, σ_i, along the i^{th} fiber is then calculated from the following equation (E is the elastic Modulus of the composite):

$$\sigma_i = E\varepsilon_m \left[1 - \frac{\cos h(kx)}{\cos h(kl_i)}\right] \quad (18)$$

where: $k = \frac{2G}{\left[r^2 \ln 2\left(E_f - E_m\right)\right]^{\frac{1}{2}}}$ while G is the shear modulus, E_f and E_m are the elastic moduli of the fiber and matrix, respectively, r is the fiber radius, and ε_m is the mean strain developed.

As Figure 1 depicts, l_i, can be calculated from the following equation:

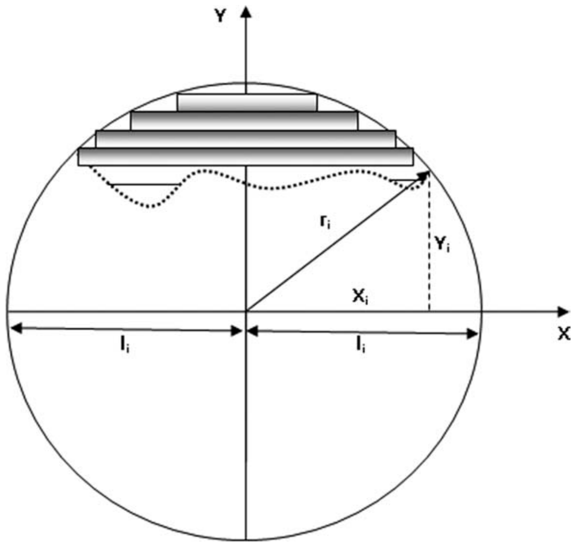

Figure 1 The proposed model subjected to tensile loading.

$$l_i = \sqrt{r^2 - y^2}$$

The average stress developed on the i^{th} fiber can then be calculated through integration as:

$$\int_{-1_i}^{1_i} \sigma_i dx = \int_{-1_i}^{1_i} E\varepsilon_m \left[1 - \frac{\cos h(kx)}{\cos h(kl_i)}\right] dx \Rightarrow$$

$$\frac{1}{2r}\int_{-r}^{r} \bar{\sigma}_i dy = \sigma_m \frac{1}{2r}\int_{-r}^{r} \frac{E_f - E_m}{E_m}\left[1 - \frac{\tan h(k\sqrt{r^2 - y^2})}{k\sqrt{r^2 - y^2}}\right] \cdot dy \tag{19}$$

where $\frac{1}{2r}\int_{-r}^{r} \bar{\sigma}_i \, dy$ is the total mean stress $\bar{\sigma}_{\text{total}}$, developed in the particle.

Then, if B is taken as:

$$B = \frac{1}{2r}\int_{-r}^{r} \frac{E_f - E_m}{E_m}\left[1 - \frac{\tan h(k\sqrt{r^2 - y^2})}{k\sqrt{r^2 - y^2}}\right] \cdot dy$$

Equation (19) can be written as:

$$\bar{\sigma}_{\text{total}} = B * \sigma_m \tag{20}$$

Now, if σ_m is replaced by the matrix ultimate strength, σ_{um}, then eq. (20), can be written as:

$$\sigma_b = B * \sigma_{\text{um}} \tag{21}$$

from which the maximum particle stress, σ_b can be calculated

The residual property model

The RPM model is a model developed by the CMG group, University of Patras, and it is used for the description of the residual behavior of polymers and polymer-matrix composites, after damage. As it was shown, the model gives accurate predictions for the residual materials properties variation irrespective of the cause of damage and of the type of material considered at the time. In the case of damage due to water absorption, impact, repeated impact, bending to a crack-like edge centred notch, and tension in nanocomposites, the RPM model predicts well the observed variation.

The final expression for the RPM model is:

$$\frac{P_r}{P_0} = s' + (1 - s')\exp(-s'M) \tag{22}$$

where P_r is the current value of the mechanical property considered at any time of the damage process, P_0 is the value of the same property for the virgin material (i.e., for the undamaged material), and M is a function depended on the source of damage and the property considered at the time. In the present case, where three-point bending tests were performed on specimens, P_r may represent one of the following properties: (i.e., bending modulus), $\sigma_{\max\ \text{fracture}}$ (i.e., stress at fracture), or $\sigma_{\max}$ (i.e., bending strength).

Also

$$s' = P_\infty / P_0 \tag{23}$$

where P_∞ is the value of the property under damage saturation conditions.

Concerning the function M, in the present case, this is given by:

$$M = \frac{a - c}{h}\ \text{(for the modulus prediction), and} \tag{24}$$

$$M = \frac{a - c}{c}\ \text{(for the strength prediction).} \tag{25}$$

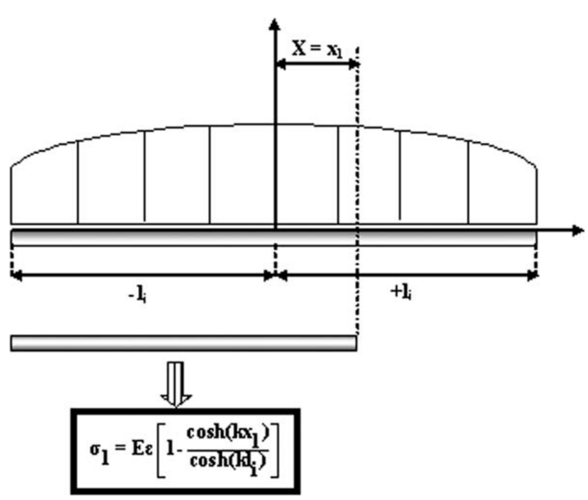

Figure 2 The stress (σ_1) in a cross section located at distance x_1 from the center of the particulate of a random fiber with length 2*li*.

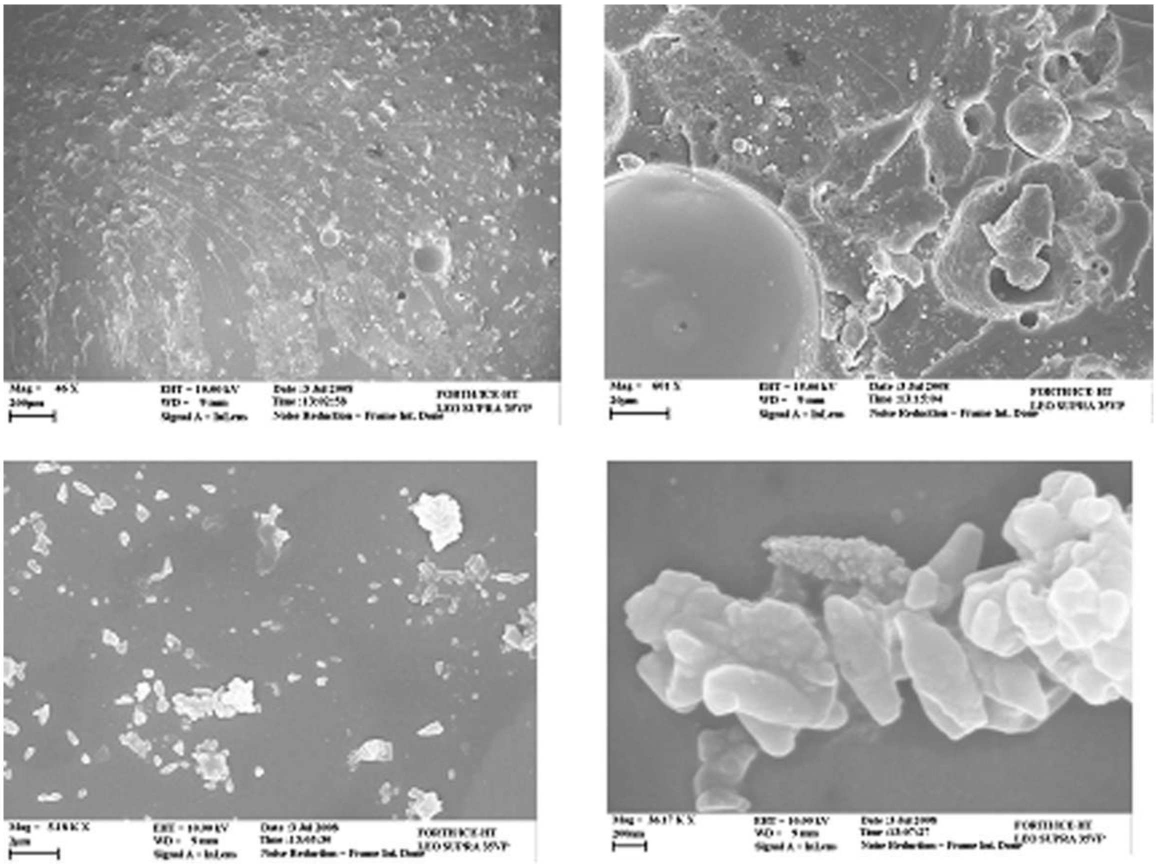

Figure 3 SEM photomicrographs for the polymer epoxy reinforced particulate reinforced with 10% v_f aluminum particles.

where: a = notch length; h = specimen thickness; c = notch length threshold; i.e., the maximum notch length where no damage effect on the material properties is observed ($c = 1$ mm).

The boundary conditions are fulfilled, since

$$M \to \infty \Rightarrow \frac{P_r}{P_0} \to s'; \tag{26}$$

$$M \to 0 \Rightarrow \frac{\mathrm{P}_r}{P_0} \to 1 \tag{27}$$

EXPERIMENTAL

Materials and manufacturing procedure

Aluminum fillers, used in the present investigation, have a rather uniform granulometry with a mean diameter of 63 μm and their density was 2.70 gr/ cm^3 at 20°C by R&G. Polymer composite formulations were prepared by mixing aluminum particles with an epoxy resin (RENLAM CY 219). Aluminum (V_f = 0%, 2.3%, 4.7%, 7.3%, 10%, 12.9%, 16%, 19.3%, 22.9%, 26.7%) particles and resin were carefully mixed for 30–40 min, to achieve uniform distribution of grains in the matrix. Proper amounts of the curing agent were then added. The aluminum-resin mixture was then placed in a vacuum pump for 3 min to reduce voids in the composite. Subsequently, the mixture was poured in plexiglas moulds (120 × 110 × 2.86 mm^3) of suitable capacity. Next, the filled moulds were placed in an oven for the curing phase. The following curing process was applied: temperature was raised at 5°C/h from ambient to 50°C and maintained constant for approximately 24 h. Plates were then removed from the molds and were subsequently cut to proper dimensions for three- point bending tests. The samples were ∼ 90 mm long, 12 mm wide and 2.85 ± 0.01 mm thick.

Then it was machined a sharp edged notch into the middle of the test specimen and then it was generated a natural crack by tapping on a new razor blade placed in the notch. Notches' length were 0, 2, 4, 6, 8, and 10 mm.

Static mechanical testing

Bending measurements were carried out with a conventional Instron type tester (INSTRON 4301), at room temperature. Specimens with a gauge length of 63 mm were tested at a constant strain rate of 1 mm/min. At least five specimens were used for each measurement and the average results were

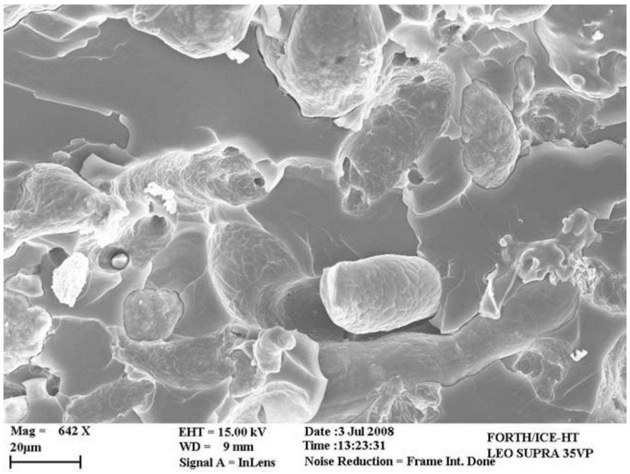

Figure 4 SEM photomicrographs for the polymer epoxy reinforced particulate reinforced with 16% v_f aluminum particles.

reported here. The repeatability of results confirms the good manufacturing conditions of the specimens as well as the appropriate selection of the curing processing conditions.

SEM fractography (scanning electron microscopy)

To study the degree of aluminum particle dispersion in the polymeric matrix, SEM photomicrographs were taken and analyzed (scanning electron microscope was JEOL JSN 5400p). Samples for SEM were coated with 5–10 nm of gold prior to examination. Figure 3 shows the tendency of aluminum (10% V_f.) particles to agglomerate. This tendency depends on both the nature of the constituent materials of the composite, the fabrication procedure followed and the conditions of manufacturing applied. From the same figures, it can also be seen that aluminum particles have perfectly spherical shape of different diameter.

Figures 4 and 5 depict polymer composites reinforced with 16% and 22.9% volume fraction of aluminum particles. From these photomicrographs, when compared with those shown in Figure 3, it can be observed that filler aggregation exists in all cases and more specifically, as the volume fraction increases, the number and the extent of agglomeration increases too.

RESULTS AND DISCUSSION

Application of the PSM model

The variation of the flexural strength of the composite under investigation with the filler volume fraction is shown in Figure 6. In the same figure, respective theoretical predictions have been plotted along with the experimental results. The most important observation is that the flexural strength decreases almost continually with the volume fraction mainly because of the agglomerations (Figs. 3–5). Also, it is clear that there is no theory predicting with accuracy the observed variation of experimentally results for all percentages of volume fraction. A final observation is that no critical filler weight fraction is observed. From all models applied, Papanicolaou PSM model and Leidner & Woodhams models predict with quite satisfactory accuracy the experimental values for the flexural strength.

Application of the IM model

Figure 7 shows the variation of the flexural modulus with filler-volume fraction. A comparison between experimental values and predictions as derived from different theories is shown. Bending Modulus experimental values are increasing continually with filler volume fraction. As can be seen, from all models applied, only Papanicolaous' Interphase model,

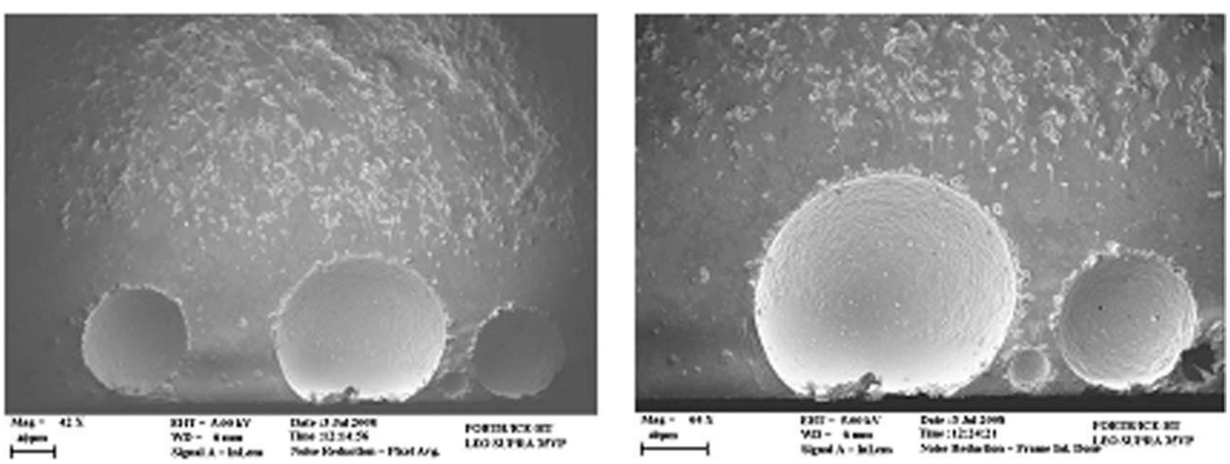

Figure 5 SEM photomicrographs for the polymer epoxy reinforced particulate reinforced with 22.9% v_f aluminum particles.

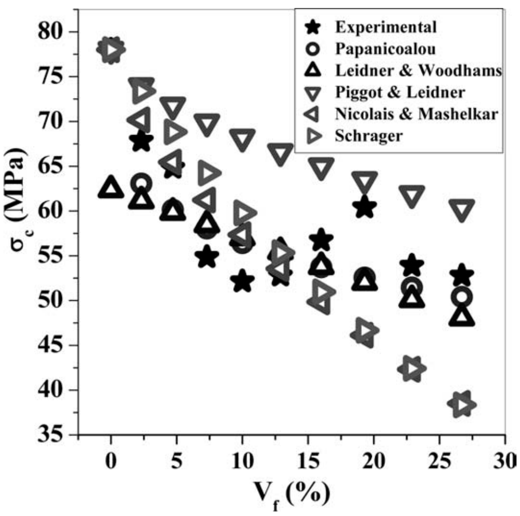

Figure 6 Comparison between experimental values and theoretical predictions as derived from several theories for the strength of the aluminum particle-epoxy matrix composites investigated.

Einsteins; and Kerners' models predict with high accuracy respective experimental results.

Application of the RPM model

Figure 8 depicts the influence of the existence of notch on specimens' strength for different volume fractions of aluminum particles. The main observation is that for all percentages of reinforcements, maximum strength is decreasing with notch's length (which was expected, because specimens' fracture

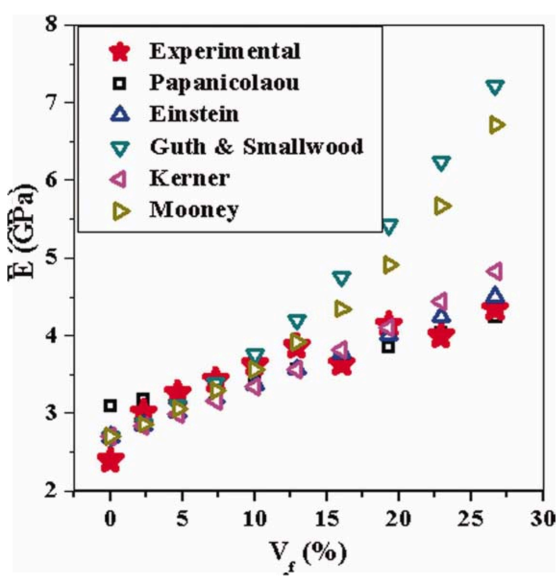

Figure 7 Comparison between experimental values and theoretical predictions as derived from several theories for the Young's modulus of the aluminum particle-epoxy matrix composites investigated. [Color figure can be viewed in the online issue, which is available at wileyonlinelibrary.com.]

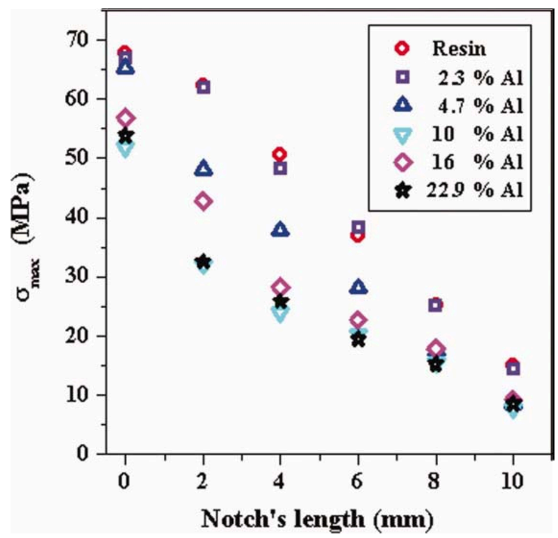

Figure 8 Variation of flexural strength with notches' length for different percentages of reinforcement. [Color figure can be viewed in the online issue, which is available at wileyonlinelibrary.com.]

energy decreases with notches' length). Another important observation is that strength is decreasing with the percentages of fillers. Thermal coefficient of epoxy and these of aluminum particles is quite different so around particles stresses were concentrated as a result strength to decrease.

In connection with the previous, in Figure 9, it can be observed that bending modulus is decreasing with notches' length for all particles volume fractions and also it is decreasing with the decrease of reinforcements' percentages. Aluminum particles have much higher modulus in comparison with

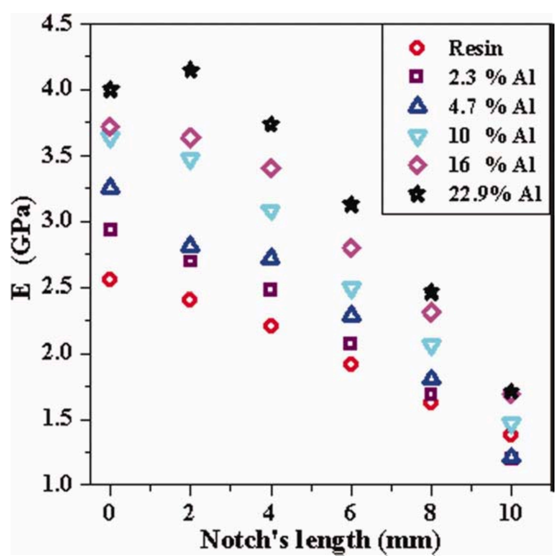

Figure 9 Variation of bending modulus with notches' length for different percentages of reinforcement. [Color figure can be viewed in the online issue, which is available at wileyonlinelibrary.com.]

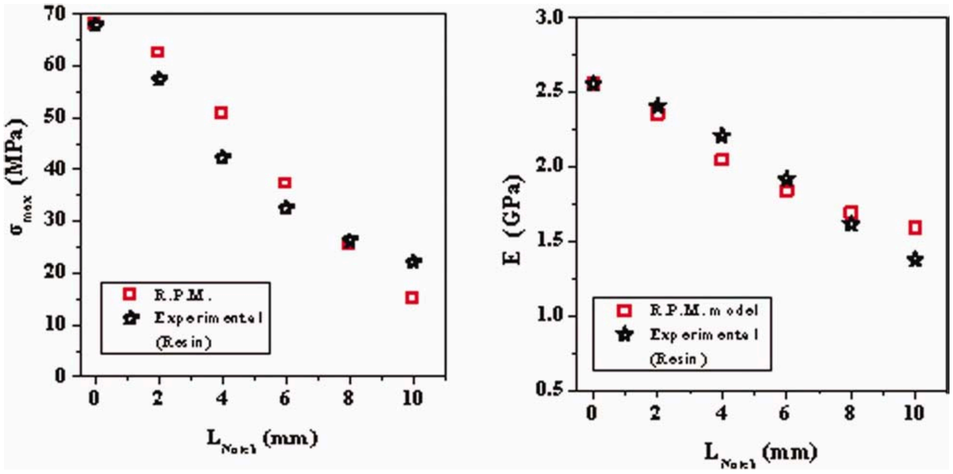

Figure 10 Comparison between experimental and analytical results as derived from the application of the RPM model for the neat resin. [Color figure can be viewed in the online issue, which is available at wileyonlinelibrary.com.]

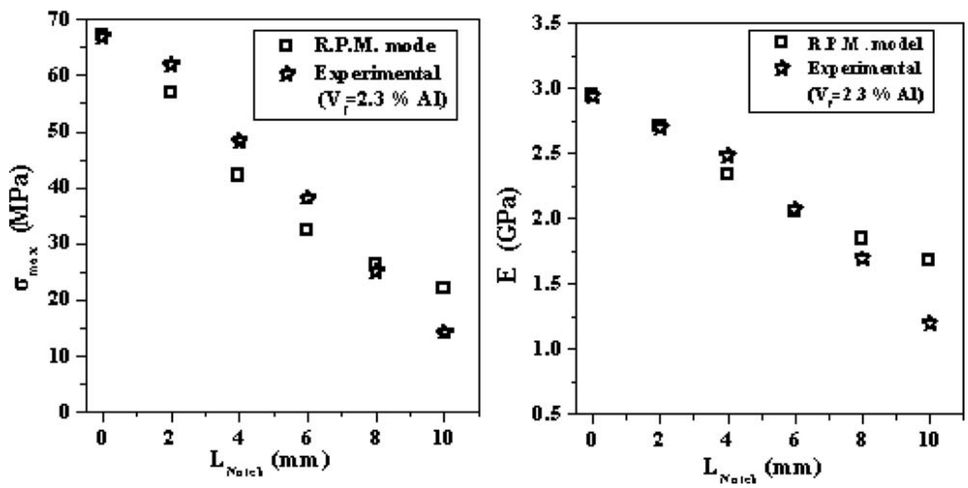

Figure 11 Comparison between experimental and analytical results as derived from the application of the RPM model for the resin reinforced with 2.3% V_f aluminum particles.

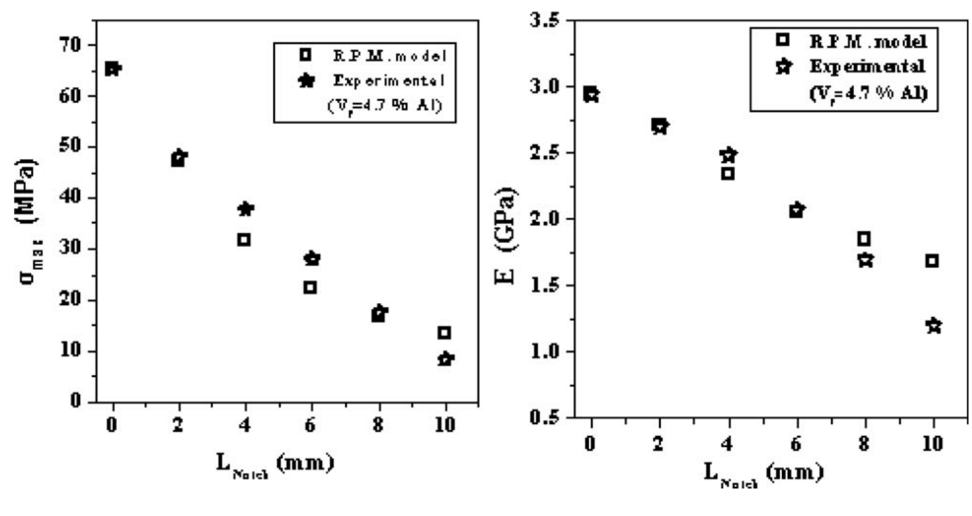

Figure 12 Comparison between experimental and analytical results as derived from the application of the RPM model for the resin reinforced with 4.7% V_f aluminum particles.

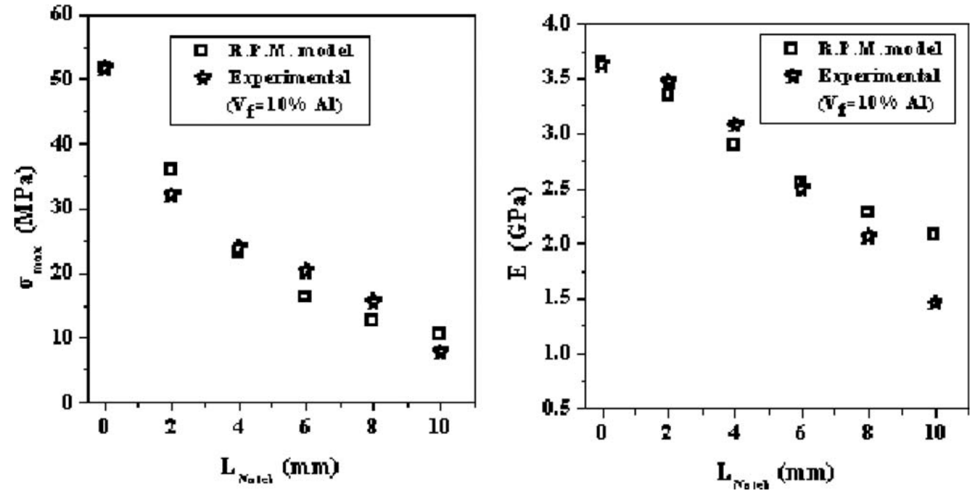

Figure 13 Comparison between experimental and analytical results as derived from the application of the RPM model for the resin reinforced with 10% V_f aluminum particles.

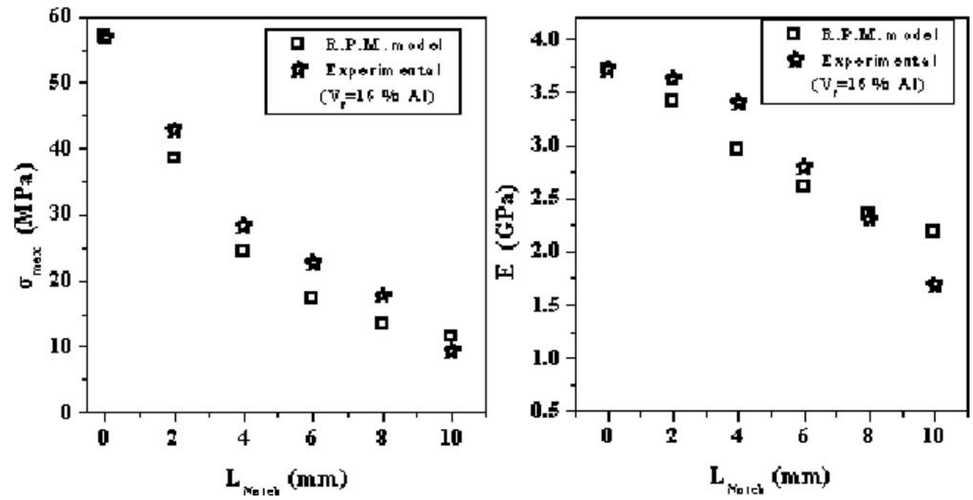

Figure 14 Comparison between experimental and analytical results as derived from the application of the RPM model for the resin reinforced with 16% V_f aluminum particles.

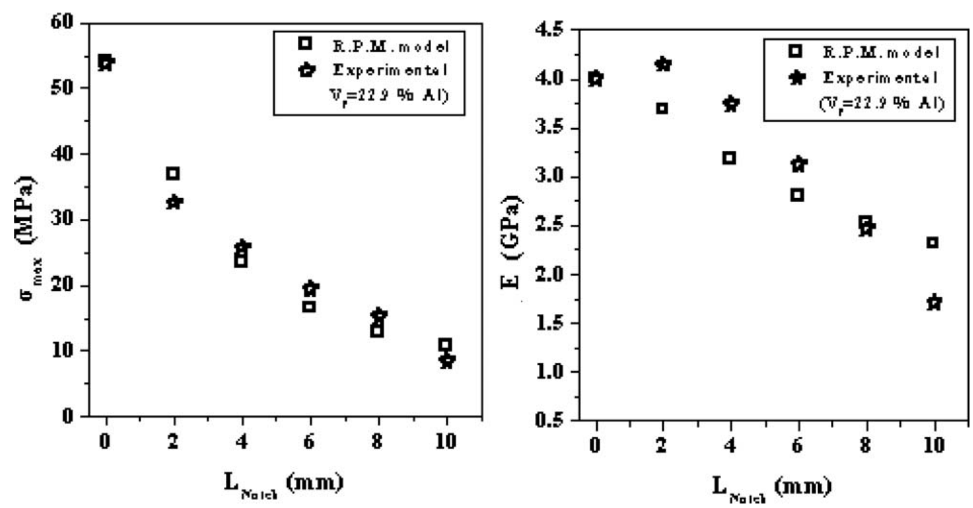

Figure 15 Comparison between experimental and analytical results as derived from the application of RPM for the resin reinforced with 22.9% V_f aluminum particles.

polymer epoxy modulus and so as volume fraction is increasing, modulus is increasing too.

Figures 10–15 depict the comparison between experimental results and analytical predictions as derived from the application of the RPM model for different notches' lengths and for different percentages of reinforcements. From all figures, it is clear that there is a fair agreement between experimental results and respective RPM predictions.

CONCLUSIONS

In the present investigation, the static bending behavior of notched and un-notched aluminum-filled epoxy particulate composites has been experimentally determined. The influence of particle-volume fraction on the static behavior of the particulate composites is thoroughly studied. A comparison between experimental and theoretical values predicted by several existing in literature models as well as by the interphase model previously developed by the first author for the evaluation of the elastic modulus in particulate composites has been done. From the whole work the following conclusions can be deduced:

Flexural strength decreases almost continuously with the filler-volume fraction due to the agglomerations existed and observed through SEM photomicrographs. Papanicolaou and Leidner & Woodhams models predict with quite satisfactory accuracy the flexural strength of particulates.

Bending modulus as derived from experiments is increasing with filler-volume fraction and that tendency was predicted by applying several different theoretical models from which only three of them predict with high accuracy respective experimental findings. These models are Papanicolaous', Einsteins', and Kerners' models.

Bending modulus is decreasing with notches' length for all particles volume fractions and also it is decreasing with the increase of reinforcements' percentages.

Finally, a fair agreement between experimental results and the RPM predictions for both the bending modulus and the flexural strength for different notches' length and percentages of reinforcements was found.

References

1. Papanicolaou, G. C.; Xepapadaki, A. G.; Kotrotsos, A.; Mouzakis, D. E. J Appl Polym Sci 2008, 109, 1150.
2. Khashaba, U. A.; Selmy, A. I.; El-Sonbaty, I. A.; Megahed, M. Compos Struct 2007, 81, 606.
3. Papanicolaou, G. C.; Kosmidou, Th. V.; Vatalis, A. S., Delides, C. G. J Appl Polym Sci 2006, 99, 1328.
4. Rao, S.; Krishna, Y.; Rao, B. N. Mater Sci Eng A 2004, 385, 429.
5. Papanicolaou, G. C.; Paipetis, S. A.; Theocaris, P. S. J Appl Polym Sci 1977, 2, 689.
6. Srivastava, V. K. Mater Sci Eng 2002, 328, 302.
7. D'Almeida, J. R. M.; De Carvalho, L. H. J Mater Sci 1998, 33, 2215.
8. Wu, G.; Tan, Y.; Yang, J.-M. Mater Sci Eng A 2007, 457, 338.
9. Chen, P.; Shen, Z.; Wang, J.-Y. Compos Sci Technol 2001, 61, 1311.
10. Kumagai, S.; Shindo, Y. Compos Mater 2004, 38, 1151.
11. Dunn, M. L.; Suwito, W. Solids Struct 1997, 34, 3873.
12. Ye, L.; Akbar, A.-A.; Lawcock, G.; Mai, Y.-W. Compos A 1998, 29, 1525.
13. Papanicolaou, G. C.; Bakos, D. J Reinforced Plast Compos 1992, 11, 104.
14. Sideridis, E.; Theocaris, P. S.; Papanicolaou, G. C. Rheol Acta 1986, 25, 350.
15. Papanicolaou, G. C.; Mouzakis, D. E.; Kosmidou, Th. V.; Economopoulos, G. Polym Compos 2006, 27, 177.
16. Einstein, A. Ann Phys 1906, 19, 289.
17. Guth, E. J Appl Phys 1945, 16, 20.
18. Smallwood, H. M. J Appl Phys 1944, 15, 758.
19. Kerner, E. H. Proc Phys Soc 1956, 69, 808.
20. Mooney, M. J Colloid Sci 1951, 6, 162.
21. Brassell, G. W. J Mater Sci 1974, 9, 307.
22. Phillips, M. G. Compos Sci Technol 1992, 43, 95.
23. Leidner, J.; Woodhams, R. T. J Appl Polym Sci 1974, 18, 2637.
24. Piggott, M. R.; Leidner, J. J Appl Polym Sci 1974, 18, 1619.
25. Nicolais, L.; Mashelkar, R. A. J Appl Polym Sci 1976, 20, 561.
26. Schrager, M. J Appl Polym Sci 1978, 22, 2379.
27. Papanicolaou, G. C.; Andreopoulos, A. G. Mater Chem Phys 1987, 18, 49.
28. Sideridis, E. P.; Papanicolaou, G. C. Rheol Acta 1988, 27, 608.